SC 1004-A (3-52)

UNCLASSIFIED

[redacted]

Ref. Sym: 5141 (607)

INVENTORIED

FEB 1 2 1959

BY URG 4722

SANDIA SYSTEMATIC DECLASSIFICATION REVIEW
DOWNGRADING OR DECLASSIFICATION STAMP

CLASSIFICATION CHANGED TO U AUTHORITY W. C. Layne
Emelda Selph 10-24-96 975 N 083
CLASSIFICATION CHANGED TO
R. T. [illegible] 10/29/96 10-21-96
PERSON MAKING DOWNGRADING DATE DATED

Technical Memorandum

INVENTORIED

MAR 8 1965

3427-1

INVENTORIED

MAR 1 1966

3428-3

SCTM 266-56-51

INVENTORIED

1963

3427-1

AN EXPERIMENTAL AND ANALYTICAL INVESTIGATION OF THE INDUCED FLOW FIELD ABOUT ROCKET MOTORS IN THE PRESENCE OF THE GROUND WITH SPECIAL ATTENTION GIVEN TO INDUCED FLOW SCALING LAWS

SANDIA SYSTEMATIC DECLASSIFICATION REVIEW

1st Review Date: 3-12-80
Authority: ☐ ADC ☒ ADD CCRP-RR
Name:
2nd Review Date: 10-21-96
Authority: ADD
Name: W Layne

Determination (Circle Number)
1 Classification Retained
(2) Classification Changed to U
3 Contains No DOE Classified Information
4 Coordinate With:
5 Contains UCAI?
6 Comments: Unclassified

Arnold L. Ducoffe*
Fred G. Blottner - 5141
V. T. Strascina - 5142
W. E. Walker - 5143

Inventoried September 1980

ABSTRACT

Experimental velocity measurements were made in the vicinity of a rocket motor. An analytical solution using image source and sink pairs is fitted to the experimental data. The resulting theory is then applied to obtain velocities at remote field points including the ground plane. An induced flow scaling law as a function of nozzle plane exit Mach number is also derived.

*Associate Professor of Aeronautical Engineering, Georgia Institute of Technology and Consultant of Aerodynamics Department, Sandia Corporation.

[redacted]

Case No. 409.10

January 2, 1957

THIS DOCUMENT CONSISTS OF 41 PAGE(S)
NO. 6 OF 18 COPIES, SERIES A

(41 pages)

[redacted]

CENTRAL M & E
CONTROL NO

UNCLASSIFIED

7.5.2

DISTRIBUTION:

1/18A - R. E. Schreiber, LASL
2/18A - Hayden Gordon, Livermore
3/18A - A. L. Ducoffe, Georgia Institute of Technology
4/18A - S. C. Hight, 5100
5/18A - M. L. Merritt, 5110
6/18A - G. E. Hansche, 5140
7/18A - T. B. Cook, 5111
8/18A - J. D. Shreve, 5112
9-11/18A - P. W. Rowe, 5141
12/18A - R. K. Smeltzer, 7221-3
13-18/18A - A. D. Pepmueller, 7223
1-2/2B REDSTONE ARSENAL

ACKNOWLEDGMENT

Recognition should be given to Aerojet-General Corporation for the splendid cooperation received while conducting tests there. Special credit should go to Mr. Tom Fehr, the test engineer, who cooperated in every way possible.

TABLE OF CONTENTS

	Page
SUMMARY	5
LIST OF SYMBOLS	6
INTRODUCTION	8
EXPERIMENTAL PROCEDURE	9
Aerojet Experiments	9
Rocketdyne Experiments	19
SCALING LAW	21
THEORY	25
RESULTS	30
CONCLUSIONS	31
APPENDIX A -- TABLE I	36
APPENDIX B -- TABLE II	37
APPENDIX C -- CALIBRATION OF A STATIC PROBE AS A FUNCTION OF ANGLE OF ATTACK	38
BIBLIOGRAPHY	41

LIST OF ILLUSTRATIONS

Figure — Page

1. -- Right Three-Quarter View of Aerojet Test Stand 10
2. -- Right-Side View of Aerojet Test Stand Showing Tuft Locations 11
3. -- Tuft Study with Ground Plane in 54-Inch Position 12
4. -- Nike Thrust Chamber with Fairing Installed 13
5. -- Right-Side View for 24-Inch Ground Plane Position Showing Tuft Directions 15
6. -- Test Setup for Aerojet Rocket Induction Study 16
7. -- Left-Side View of Test Stand Showing Static Probe Orientation 17
8. -- Left-Side View of Test Stand Showing Rocket Exhaust and Smoke Flow 18
9. -- Test Setup for Rocket Induction Study at Rocketdyne 20
10. -- Analytical Induced Flow Scale Factor for Scaling Aerojet Data as a Function of the Nozzle Exit Plane Mach Number 26
11. -- Image Sink System 28
12. -- A Comparison of the Streamline Directions Created by an Image Sink Pair Located at $x/d_e = \pm 5$, $y/d_e = 0$ and the Flow Directions Given by Tuft Studies (Ref. Fig. 5) 32
13. -- Induced Flow Field About the Nuclear Rocket Based on an Image Sink Pair Whose Strength and Position Are Determined by Scaling of Aerojet Test Results 33
14. -- Induced Flow About the Nuclear Rocket Based on an Image Sink Whose Strength and Position Are Determined by Scaling of Aerojet Test Results 34
15. -- Static Pressure Error as a Function of Flow Inclination and Velocity on a 1/4-Inch Diameter Static Probe 39

SUMMARY

This paper presents the results of an experimental and analytical investigation of the induced flow field about rocket motors. Tests were run in which the induced flow about a 2600-pound thrust Nike rocket motor at Aerojet (Azusa, California) and about a 135,000-pound thrust chamber at Rocketdyne (Canoga Park, California) was measured. In each case the tests were set up to simulate tests on a rocket whose exhaust was directed vertically upwards with the rocket nose resting on the ground. Velocity measurements using static probes were made outside the rocket shell slightly forward of the nozzle exit plane. Tuft studies were also made to determine induced flow directions.

An analytical theory using image source and sink pairs, placed on the thrust axis downstream of the nozzle exit plane, is derived and shown to give a good qualitative fit to the experimental data. The source and sink distribution is then used to compute the velocity distribution at remote field points including points on the simulated ground plane. In addition a scaling law dependent on the nozzle exit plane flow characteristics is derived. The resulting empirical theory is then applied to the proposed nuclear rocket tests and permits the qualitative calculation of the induced flow in the immediate vicinity and also at remote field points about the nuclear rocket motor.

LIST OF SYMBOLS

a	location of sink along the x axis, ft
c	speed of sound of air, ft/sec
c_η	speed of sound of exhaust gases for the η rocket, ft/sec
c_e	speed of sound of exhaust gases, ft/sec
c_o	stagnation speed of sound, ft/sec
c_{o_η}	stagnation speed of sound for the η rocket gaseous medium, ft/sec
c_p	specific heat at constant pressure
c_v	specific heat at constant volume
d_e	nozzle exit diameter, in.
i	subscript which indicates summation over sink positions; also the imaginary unit, $\sqrt{-1}$
j	subscript which identifies the magnitude and location of measured velocities
l	mixing length, ft
m	sink strength
p	static pressure, lbs/sq ft
p_a	ambient air pressure, lbs/sq ft
p_e	nozzle exit static pressure of exhaust gases, lbs/sq ft
p_o	stagnation pressure, lbs/sq ft
Δp	static pressure error, lbs/sq ft
u	velocity component in x direction, ft/sec
v	velocity component in y direction, ft/sec
x	coordinate
y	coordinate
A^*	area of nozzle where Mach number is unity
A_e	area of nozzle exit
H	total head pressure, lbs/sq ft
M	molecular weight of exhaust gases at nozzle exit
M_e	Mach number of exhaust gases at nozzle exit
P	factor $= x^2 - 2ax + y^2 + a^2$
Q	factor $= x^2 + 2ax + y^2 + a^2$
R	gas constant
T	thrust, lbs
T_a	ambient air temperature, degrees Rankine
T_e	nozzle exit temperature of exhaust gases, degrees Rankine
T_o	stagnation temperature, degrees Rankine
V	induced velocity, ft/sec; also velocity, ft/sec

$V_{Aerojet}$	velocity of induced flow created by the Aerojet rocket exhaust
$\lvert V \rvert$	absolute value of induced velocity, ft/sec
V_e	nozzle exit velocity of exhaust gases, ft/sec
V_j	local jet wake velocity at any jet cross section, ft/sec
V_η	velocity of induced flow created by the η rocket exhaust
W	complex potential $= \varphi + i\,\psi$
z	field point in complex plane $(= x + i\,y)$
$\bar{z}$	conjugate of z $(= x - i\,y)$
γ	ratio of specific heats, $c_p/c_v = 1.4$
η	subscript indicating properties of the η rocket
θ	flow inclination measured with respect to the horizontal or x axis
π	factor = 3.1416
ρ	mass density of air, slugs/ft^3
ρ_a	mass density of ambient air, slugs/ft^3
ρ_e	mass density of exhaust gases, slugs/ft^3
ρ_j	local jet wake mass density at any jet cross section, slugs/ft^3
ρ_o	stagnation mass density, slugs/ft^3
$\sum_i$	indicates summation over variables having "i" as a subscript
τ	shear stress, lbs/sq ft
Ω_{M_e}	induced flow scale factor at nozzle exit Mach number, M_e
$\Omega_{M_e = 1.5}$	induced flow scale factor at nozzle exit Mach number, $M_e = 1.5$
φ	velocity potential
ψ	stream function
∇^2	scaler operator derived from dot product of $\nabla \cdot \nabla = \frac{\partial^2}{\partial x^2} + \frac{\partial^2}{\partial y^2}$
∂	indicates a partial derivative

UNCLASSIFIED
[redacted]

AN EXPERIMENTAL AND ANALYTICAL INVESTIGATION OF THE INDUCED FLOW FIELD ABOUT ROCKET MOTORS IN THE PRESENCE OF THE GROUND WITH SPECIAL ATTENTION GIVEN TO INDUCED FLOW SCALING LAWS

INTRODUCTION

During the Spring of 1956, a request from the Los Alamos Scientific Laboratory (LASL) was made of the Sandia Corporation to study the induced flow field external to large rockets. The reason for this request was based on LASL plans to develop a large rocket or η rocket which is tentatively scheduled to be fired in the near future. Informal plans indicate the η rocket will be mounted with the rocket axis perpendicular to the ground and the exhaust being directed vertically upwards. The exit plane of the rocket nozzle would be approximately 15 feet from the ground with nozzle exit diameters varying between 1 and 3 feet, yielding exit Mach numbers in the range between unity and four. The information required is essentially twofold: (a) what is the induced flow field in the vicinity of the rocket, and (b) how far out must one travel along the ground before the induced ground velocity decays to essentially zero? The answer to (a) would determine for LASL the local wind velocities to which instrumentation would be subjected, and (b) would determine the size of the concrete pad required to prevent the entrainment of dust.

The solution of this problem was undertaken in June 1956. The plan to attack the problem involved measuring flow fields around large and small rockets as well as the development of a simple analytical theory based on the experimental data. Testing time was made available at Rocketdyne (a division of North American Aircraft) in Canoga Park, California, and at Aerojet in Azusa, California. The rocket at Rocketdyne had a thrust of approximately 135,000 pounds and that at Aerojet of the order of 2600 pounds. These were the only available rockets which could be instrumented during July of 1956. This range of thrusts was considered suitable since the proposed η rocket would have a thrust range between 10,000 and 200,000 pounds.

Attempts to develop a simple theory for the induced flow field about a rocket met with little success for two important reasons. First, the solution was desired by LASL by August 1, 1956; and second, the available literature indicated that studies of the jet structure of free jets had been made on a limited scale with little or no attention paid to the flow field outside the jet boundaries. It was then decided that the theory would be set up after the experimental data were available in order that intuition and experimental evidence could be combined to give some clue as to the physical processes involved.

UNCLASSIFIED
[redacted]

EXPERIMENTAL PROCEDURE

Aerojet Experiments

Measurements of the induced flow field external to a Nike thrust chamber delivering 2600 pounds of thrust were made at the Aerojet Proving Grounds in Azusa, California, during the period 16-19 July, 1956. Photographs of the experimental equipment are shown in Figs. 1 and 2. The ground plane which simulates the actual ground for the LASL η rocket tests was constructed of 3/4-inch plywood measuring 16 x 16 feet. In Fig. 1 the ground plane is located 54 inches forward of the thrust chamber exit plane. During the latter part of the test program the ground plane was moved to a position 24 inches forward of the nozzle exit plane. The actual ground level is 55 inches from the thrust axis. Since pressure measurements were to be made in the vertical plane containing the horizontal thrust axis and above the thrust chamber it is assumed that the influence of the ground is negligible. This fact was substantiated during the test program when it was learned that the velocity on the simulated ground plane in the 54-inch position was essentially zero.

The test program consisted of six runs which are summarized in Table I in Appendix A. The initial run with the ground plane in the 54-inch position consisted of a tuft study in order to determine flow directions. Figure 2 shows the tufts located in nine vertical rows (the first row being in the nozzle exit plane) with 6-inch spacing. The first horizontal row of tufts was located 6 inches above the thrust axis with each succeeding horizontal row being spaced in 3-inch intervals. The tuft data (Figs. 2 and 3) indicate that the flow angles are very steep, varying from approximately 45 degrees near the chamber surface to as high as 65 degrees at 18 inches above the thrust axis. After viewing the tuft pictures it was suspected that the induced velocities might be so low that the angles shown in Fig. 3 were exaggerated because of the effect of gravity on the wool tufts. It was decided that the flow angles indicated by the tufts should be corroborated using smoke. At the suggestion of Aerojet (Mr. Tom Fehr) a simple smoke generator was built using titanium tetrachloride. The generator, as shown in Fig. 8, consists of a pan whose sides were approximately 1-1/2 inches high and into which liquid titanium tetrachloride is poured. The liquid immediately forms a dense white smoke and a few cubic centimeters will continue to produce smoke for about 15 minutes. It should be noted that titanium tetrachloride vapors are extremely toxic; thus extreme care is required. Prior to the running of the smoke, data speculation as to the effect of the support around the nozzle exit arose. It appeared that the flow direction near the nozzle exit might be exaggerated because of the sharp change in flow direction caused by the supporting collar. A fairing over the upper half of the thrust chamber was added, and the change in external chamber geometry can be seen by comparing Figs. 3 and 4. The results of the smoke tests indicated

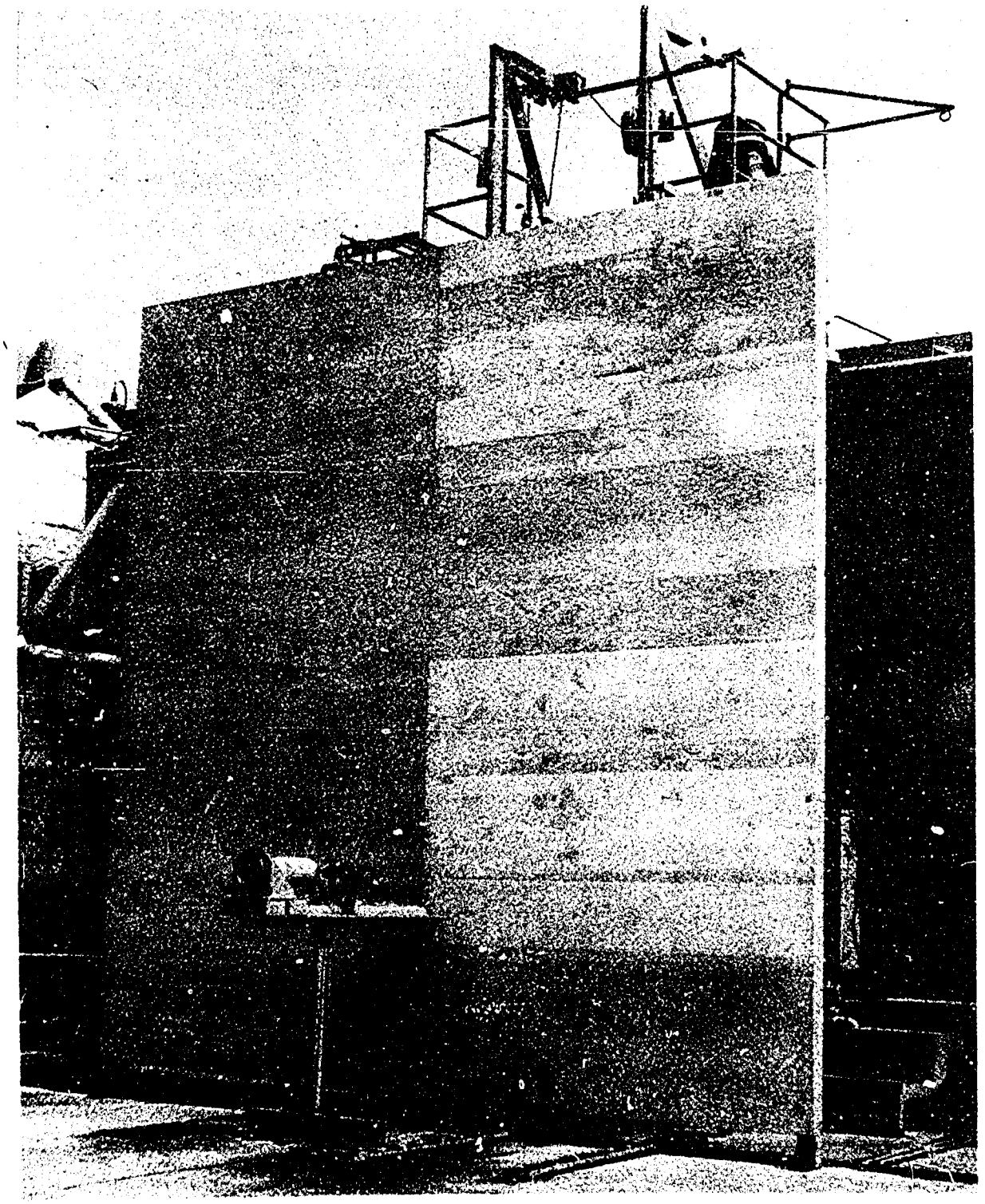

FIG. 1 RIGHT THREE-QUARTER VIEW OF AEROJET TEST STAND

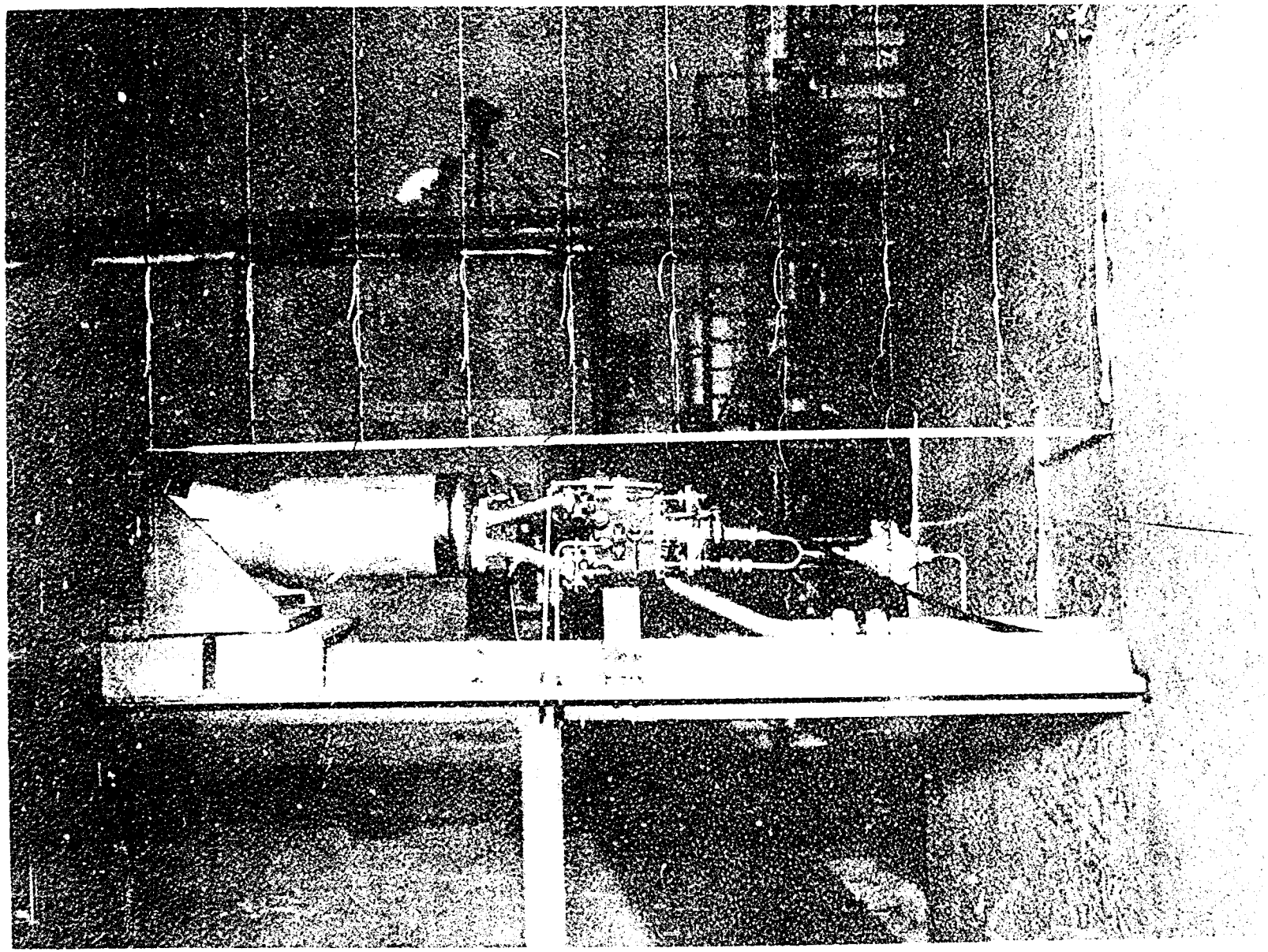

FIG. 2 RIGHT-SIDE VIEW OF AEROJET TEST STAND SHOWING TUFT LOCATIONS

Ref. Sym: 5141 (607)

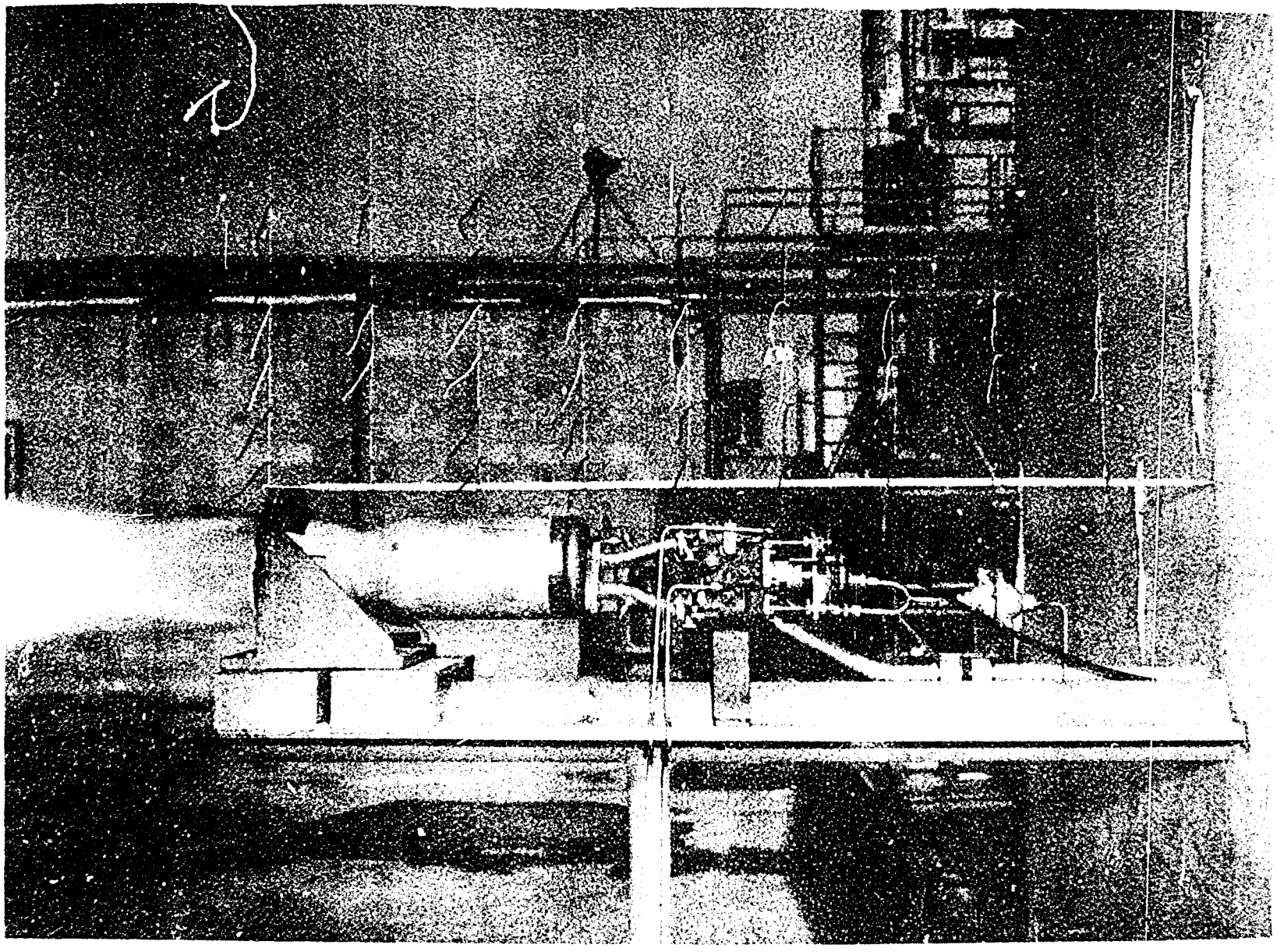

FIG. 3 TUFT STUDY WITH GROUND PLANE IN 54-INCH POSITION

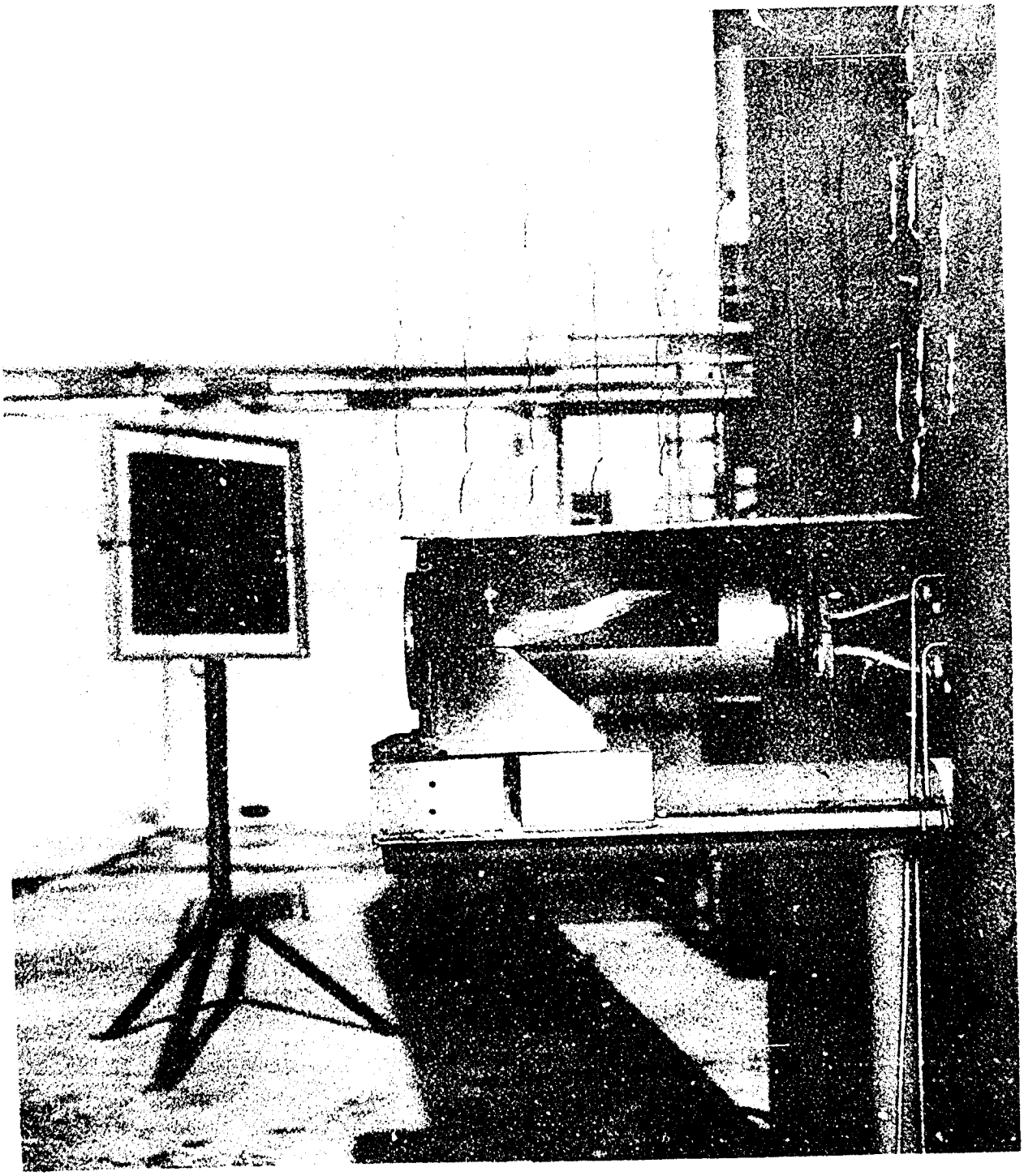

FIG. 4 NIKE THRUST CHAMBER WITH FAIRING INSTALLED

that the tuft data was essentially correct. A typical photograph of the smoke flow is shown in Fig. 8. The results of the tuft data for the 54-inch ground plane position are obtained by comparing Figs. 2 and 3 and data for the 24-inch ground plane position are shown in Figs. 4 and 5. Being assured of the flow angularity external to the thrust chamber, static probes were mounted in the vertical centerline plane above the thrust chamber. Each probe contained eight static ports equally spaced on the periphery of the 1/2-inch diameter tube. These ports were located 8-tube diameters aft of the intersection of the hemispherical nose and the cylindrical tube and approximately 8-diameters forward of the support which anchored the probe to the test stand. Unfortunately, the probes could not be aligned with the flow since those in the vicinity of the exit plane would have extended into the hot exhaust gases and those in the forward positions could not be inclined because of space limitations. Figure 6 represents a schematic diagram showing the orientation of the five static probes, the three flush orifices in the ground plane, and the two ground plane positions. Figure 7 shows the no-flow condition with the static probes mounted on the test stand, whereas Fig. 8 represents a typical run.

The pressure data were measured on a multitube manometer board (inclined at 15 degrees to the horizontal) using alcohol (dyed red) as the fluid medium. Each run was essentially 20 seconds in duration and the manometer board was photographed at 1-second intervals during the course of each run. Pressures were recorded by the framing camera for two runs wherein the static probes were mounted as shown in Fig. 6 and the ground plane located in the two positions indicated in Fig. 6. Since the flow angles over the static parts varied from 45- to approximately 65-degrees, corrections to the measured values of static pressure were necessary. In order to obtain these corrections an experimental program on the effect of angle of attack on static pressure measurements on a static probe was initiated and run in the 6-inch open jet tunnel at Sandia Corporation. A description of the program and the results are reported in Appendix B. The Aerojet velocity, corresponding to the corrected pressured, and the flow angle at each probe are given below. The location of the centroid of the static ports for each probe is referenced to an origin of coordinates in the ground plane described by the intersection of the thrust axis and the ground plane (with the ground plane in the 24-inch position). The static probe data for the two ground plane positions were essentially the same. For the case of the 54-inch ground plane position the manometer fluid gave no indication of a ground plane velocity. However, for the 24-inch position there was a slight movement of the manometer fluid. In analyzing the ground plane data for this latter case it was realized that the manometer lacked enough sensitivity to record small pressure differences. Thus the data on the ground plane were considered unreliable and are not recorded herein.

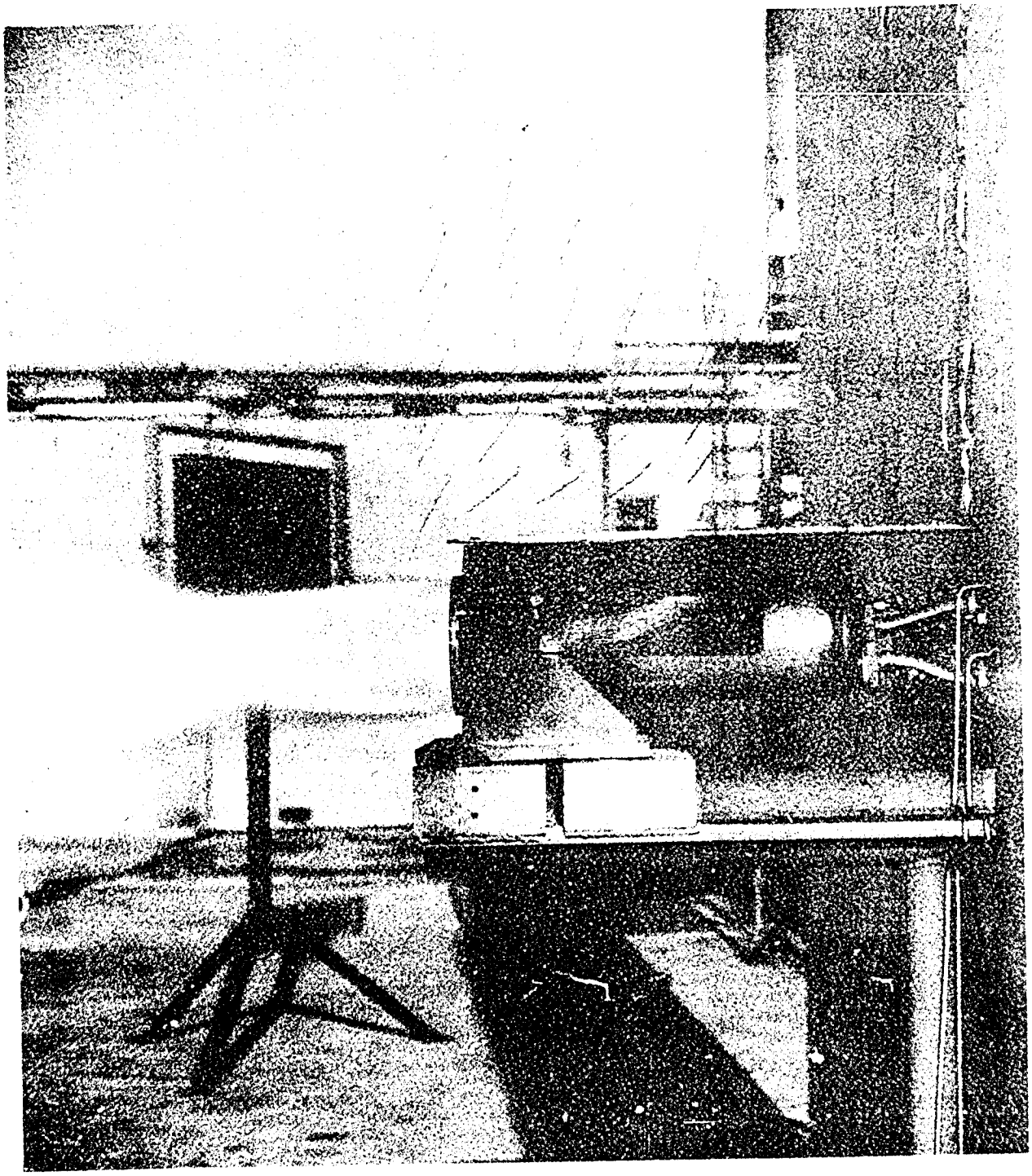

FIG. 5 RIGHT-SIDE VIEW FOR 24-INCH GROUND PLANE POSITION SHOWING TUFT DIRECTIONS

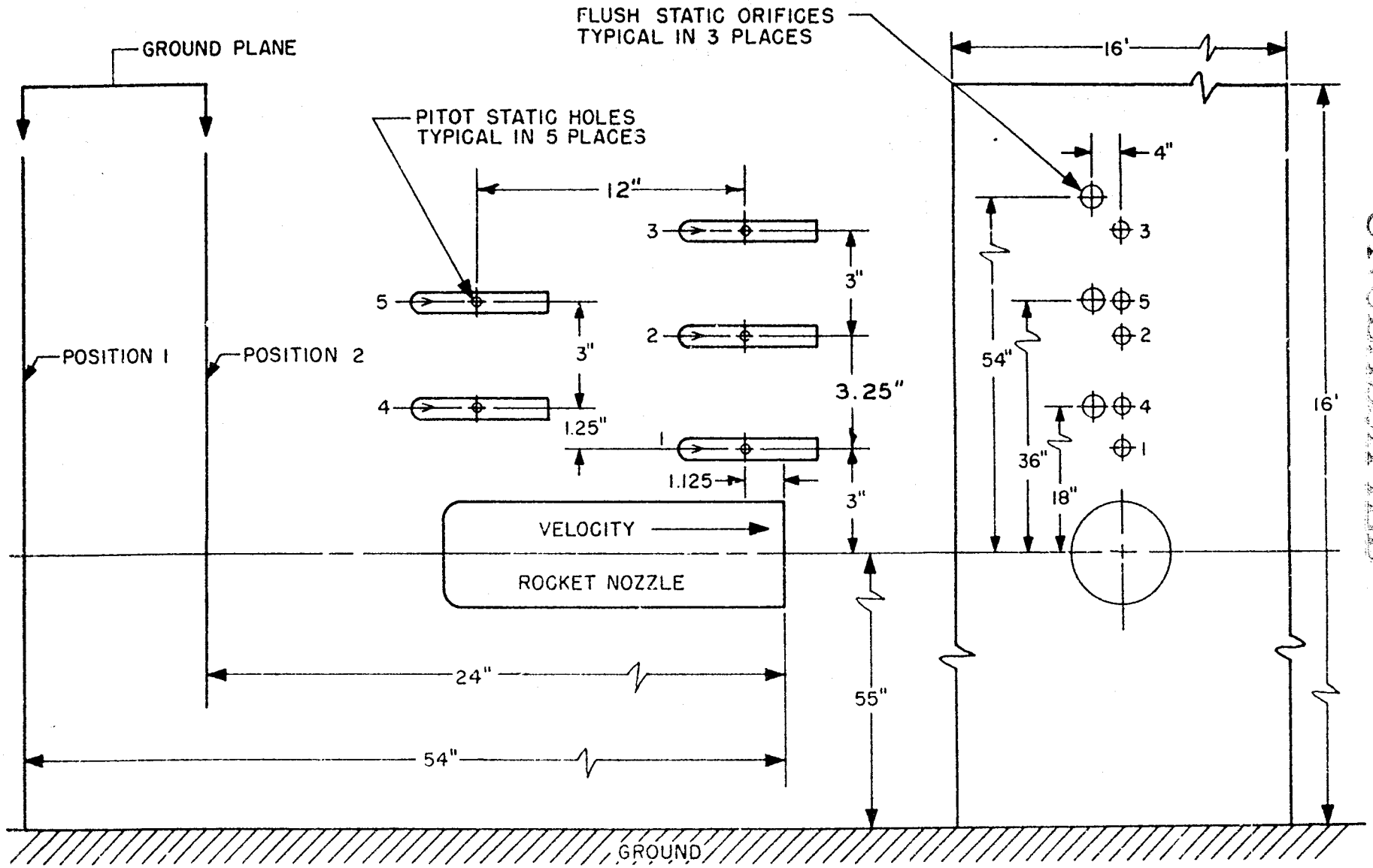

TEST SETUP FOR AERO-JET ROCKET INDUCTION STUDY

Ref. Sym: 3141 (607)
FIG. 6

UNCLASSIFIED

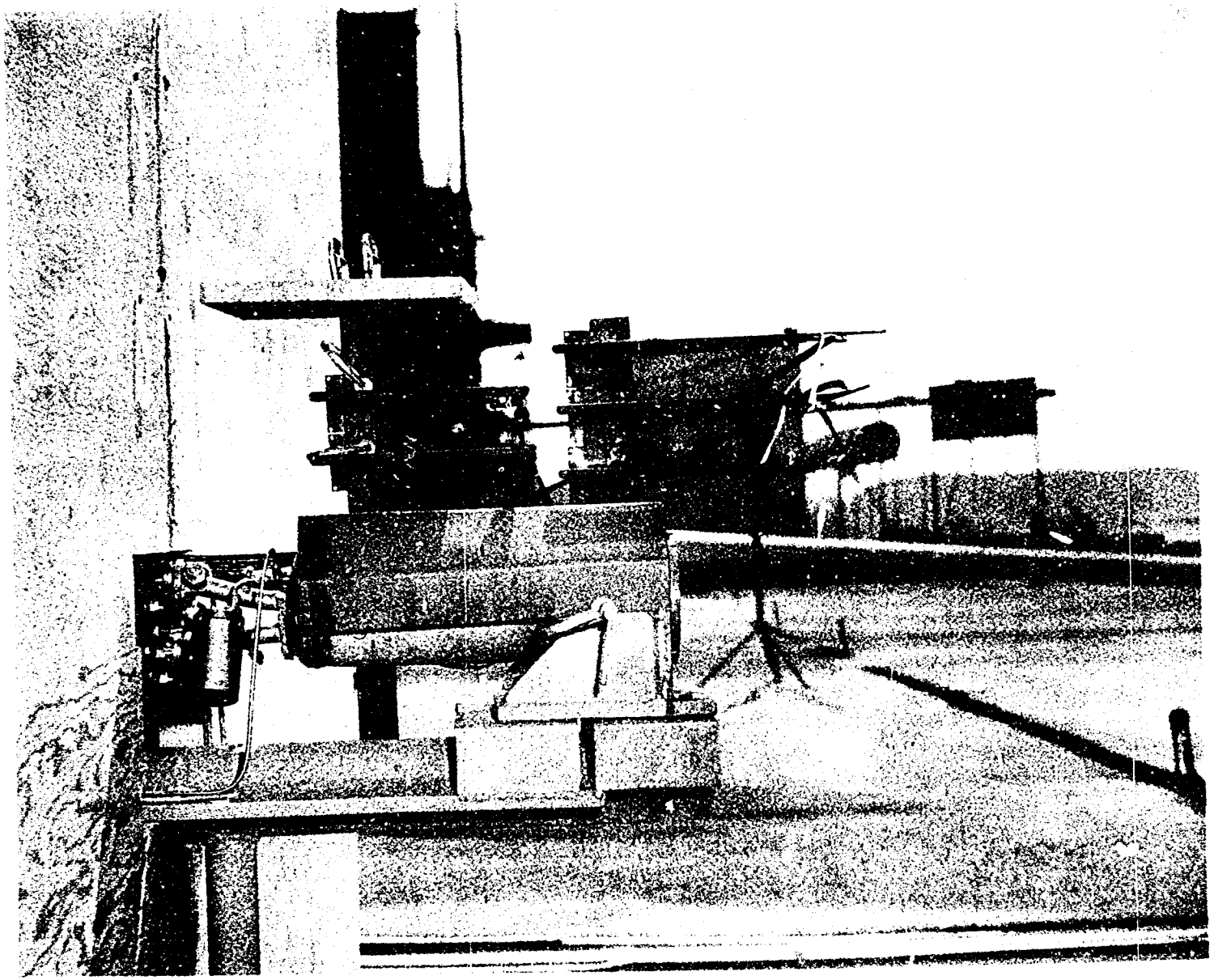

FIG. 7 LEFT-SIDE VIEW OF TEST STAND SHOWING STATIC PROBE ORIENTATION

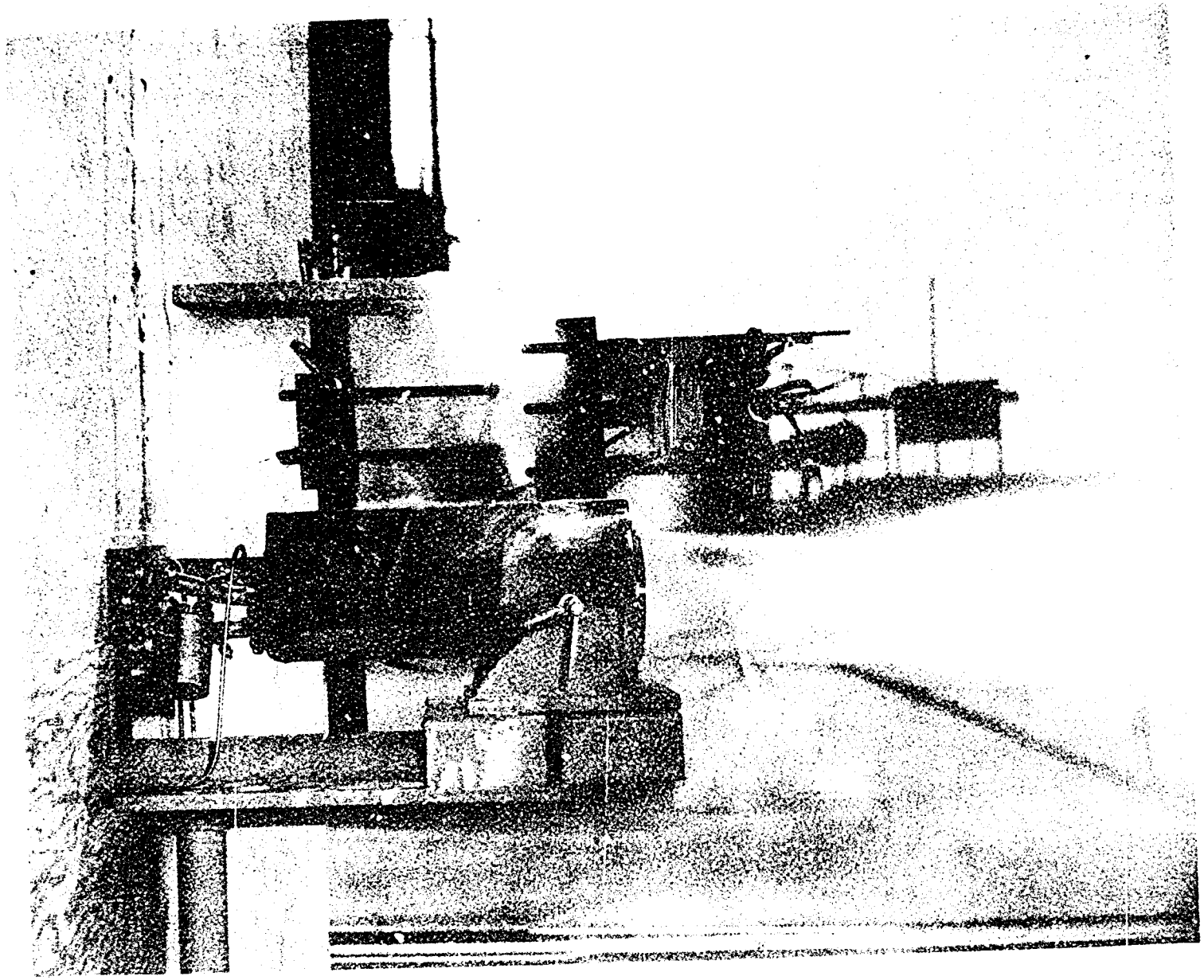

FIG. 8 LEFT-SIDE VIEW OF TEST STAND SHOWING ROCKET EXHAUST AND SMOKE FLOW

Velocities and Flow Angles at Static Probes
(24-inch ground plane position)

Static Probe (Ref. Fig. 6)	x (ft)	y (ft)	θ (degrees)	V (ft/sec)	u (ft/sec)	v (ft/sec)
1	1.98	0.52	-50	31.8	20.4	-24.4
2	1.98	0.792	-63	19.8	9.0	-17.6
3	1.98	1.052	-62	13.0	6.1	-11.5
4	0.99	0.625	-45	17.7	12.5	-12.5
5	0.99	0.875	-57	14.3	7.8	-12.0

It should be noted that the flow angles, θ, were measured in Fig. 5. A further point which should be made involves the time of day during which the experiments were run. At the outset it was apparent that the induced velocities would be low. Thus the experiments had to be run early in the morning when the prevailing winds are practically nonexistent.

Rocketdyne Experiments

Measurement of the flow field external to a 135,000-pound rocket thrust chamber was undertaken at Rocketdyne during the period 20-26 July, 1956. The measurements were made on the Horizontal Test Stand (HTS). A schematic drawing of the static probe and ground plane orientation is shown in Fig. 9.

Tufts were installed above the thrust chamber in the vertical centerline plane. Photographs of the first run indicated that the igniter flame, which envelopes the entire thrust chamber prior to firing the main stage, had burned off all the tufts. A second attempt using aluminum foil tufts had the same results. A third run using glass tape was successful, but the photography was so poor that only a qualitative idea as to the flow angles could be obtained. The static probes were installed as shown in Fig. 9 and the program proceeded. The pressure data were measured using sensitive altimeters mounted in a plywood panel board and connected to the probes by means of 1/8-inch ID copper tubing. The data were recorded with a 16-mm movie camera which was focused on the sensitive altimeters. In addition, a television camera was focused on the altimeters in order that the data could be observed on a screen located in the control room. During the first pressure run, observation of the altimeters indicated that most of the hands were moving in the wrong direction. That is, the altimeters indicated a decrease in altitude instead of an increase in altitude. This corresponds to a higher-than-ambient static pressure at the static ports. This was obviously erroneous. In addition, the movie camera jammed so no data were available to check the visual observations. A second pressure run was made with visual observations similar to those in the first run. At the end of the second run we were informed that one further run

UNCLASSIFIED

PROBES	
NO.	ANGLE
2	G.P.
3	G.P.
4	G.P.
5	45°
6	↑
7	
8	
9	
10	↓
11	45°
12	25°
13	45°
14	60°

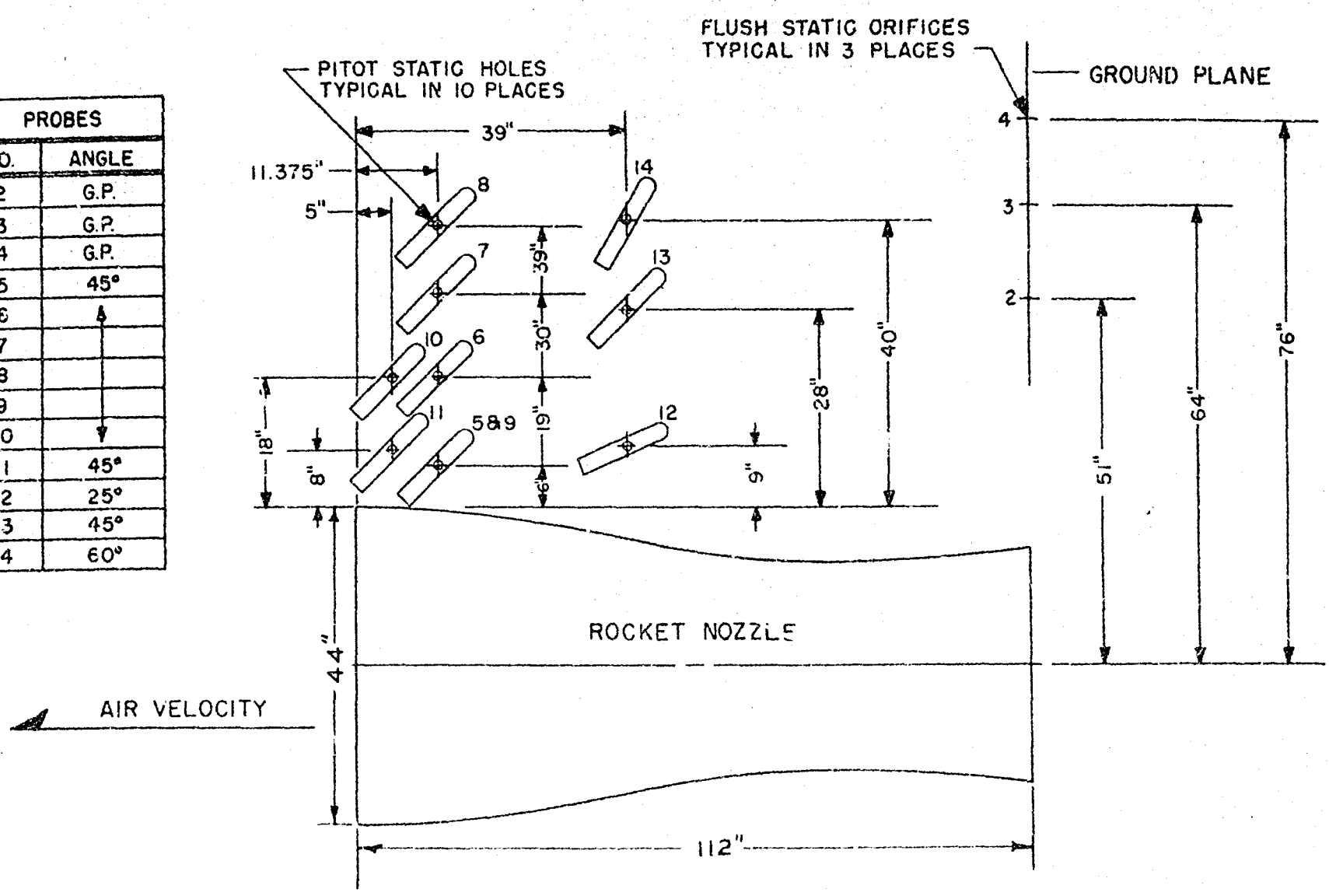

TEST SET-UP FOR ROCKET INDUCTION STUDY AT ROCKETDYNE

UNCLASSIFIED

Ref. Sym: 5141 (607)

FIG. 9

was available. Photographic data of the altimeters from the second pressure run substantiated the visual observations. The third run was made late at night, the result of which was negative since the cameras either jammed or were not loaded or not exposed correctly. It was realized after viewing the pictures in Albuquerque that the failure to record accurate data was due to water clogging the static ports and lines leading to the altimeters. The origin of the water stems from the fact that the thrust chamber and its environs are sprayed with water immediately prior to and after the thrust chamber is fired. This is done in order to reduce the fire hazard. The net result is that no data of value were recorded from the static probes. Flush orifices 2 and 4 on the ground plane (Fig. 9) indicated pressures which are equivalent to velocities of approximately 40 ft/sec but orifice 3 on the ground plane showed essentially zero velocity. On the basis of this variation between the ground plane data one concludes that the ground plane data is at best, questionable.

SCALING LAW

At the outset it was realized that very little published information exists on induced flow scaling laws for rockets. One possible cause of inflow into the exhaust jet is the shear caused by the relative velocity of the gases in the jet wake and the ambient air. A well-known formula for shear stress is given by

$$\tau = \rho l^2 \left|\left(\frac{\partial u}{\partial y}\right)\right| \left(\frac{\partial u}{\partial y}\right) \tag{1}$$

where τ is the shear stress, ρ the density, l a characteristic length called the mixing length, and $\frac{\partial u}{\partial y}$ the velocity derivative normal to the direction of the shear stress. The absolute sign on one of the velocity derivatives is used in order to determine the sign or direction of the shear stress. Since the velocity appears as a squared term in the shear stress formula one speculates that probably the important scaling factor for the external flow field about a rocket would be the nozzle exit plane dynamic pressure, that is, $1/2\ \rho_e V_e^2$. This factor also corresponds to one half the thrust per unit area. Since stress corresponds to pressure and pressure is proportional to the square of the velocity, it appears that the scaling factor for the velocities in the external flow field would be a function of the square root of the jet dynamic pressure, that is, $\sqrt{1/2\ \rho_e V_e^2}$. After considerable discussion it was decided that the above-mentioned scaling law, in the absence of any information whatsoever, should prove adequate for our purposes. Thus the scaling law states that the dynamic pressure of the induced flow field should be proportional to the dynamic pressure of the exhaust gases in the exit plane of the rocket thrust chamber. The proportionality factor is not known and could not be determined from the present test data. However, a paper[1] published recently indicates that when a gas issues into a still gaseous medium the dynamic pressure of the local inflow at any jet

wake cross section of unit length can be approximated by the ratio of the square root of the dynamic pressures, i.e.,

$$\frac{1/2\ \rho\ V^2}{1/2\ \rho_j\ V_j^2},$$

where ρ_j and V_j are the local wake values of the jet density and jet velocity at any cross section of the jet and ρ and V are the local values of the density and velocity of the inflow across the wake boundary. Actually the local jet wake velocity and density vary over the jet cross section and an average integrated value would be used. The use of the scaling law from Ref. 1 is only strictly applicable in the immediate neighborhood of the jet boundaries. However, it seems apparent that this law could be used qualitatively in the external flow field since external to the jet boundaries the flow can be described by a potential function. The problem which arises in applying the data from Ref. 1 is that very little knowledge is available for the determination of the jet wake structure, that is, the cross-sectional velocity and density distribution. If enough information on jet structure could be obtained then the inflow velocities at the jet boundary could be determined. These inflow velocities would then serve as boundary conditions for determination of a three-dimensional sink distribution (placed on the thrust axis) from which the external flow field remote from the jet boundaries could be calculated.

On the basis of Ref. 1 and discussions with Aerojet it has been decided that the velocities in the induced flow field external to the jet boundaries and the thrust chamber would be scaled using the dynamic pressure in the nozzle exit plane of the jet exhaust. The method to be used is described briefly as follows. The experimental data measured by the five static probes at Aerojet would be scaled as shown below:

$$\frac{\left(\rho_a V^2\right)_\eta}{\left(\rho_a V^2\right)_{Aerojet}} = \frac{\left(\rho_e V_e^2\right)_\eta}{\left(\rho_e V_e^2\right)_{Aerojet}} \tag{2}$$

where

$\left(\rho_a V^2\right)_\eta$ is the induced dynamic pressure for the η rocket test

$\left(\rho_a V^2\right)_{Aerojet}$ is the induced dynamic pressure for the Aerojet tests

$\left(\rho_e V_e^2\right)_\eta$ is the exit plane dynamic pressure for the η rocket

$\left(\rho_e V_e^2\right)_{Aerojet}$ is the exit plane dynamic pressure at Aerojet.

Stated more simply we write

$$\frac{V_q}{V_{Aerojet}} = \sqrt{\frac{\left(\frac{\rho_e}{\rho_a} V_e^2\right)_q}{\left(\frac{\rho_e}{\rho_a} V_e^2\right)_{Aerojet}}} = \frac{\left(V_e\sqrt{\frac{\rho_e}{\rho_a}}\right)_q}{\left(V_e\sqrt{\frac{\rho_e}{\rho_a}}\right)_{Aerojet}} . \qquad (3)$$

A summary of the ambient air properties and jet exhaust properties in the exit plane of the Aerojet Nike thrust chamber are given below.

1. Thrust, $T = 2600$ lbs
2. Ambient air pressure, $p_a = 2077$ lbs/sq ft
3. Ambient air temperature, $T_a = 549^\circ$ Rankine
4. Ambient air density, $\rho_a = 0.00243$ slugs/ft^3
5. Molecular weight of exhaust gases, $M = 25$*
6. Nozzle exit pressure of exhaust gases, $p_e = 2077$ lbs/sq ft*
7. Nozzle exit temperature of exhaust gases, $T_e = 2960^\circ$ Rankine*
8. Nozzle exit velocity of exhaust gases, $V_e = 5500$ ft/sec*
9. Nozzle exit diameter, $d_e = 25$ inches*

From the above data the value of $\left(V_e\sqrt{\frac{\rho_e}{\rho_a}}\right)_{Aerojet}$ is found to be 2280 ft/sec.

The ambient air properties in the test area where the q rocket will be fired are given below as follows:

1. Ambient air pressure, $p_a = 1872$ lbs/sq ft,
2. Ambient air temperature, $T_a = 530^\circ$ Rankine,
3. Ambient air density, $\rho_a = 0.00206$ slugs/ft^3.

The properties of the gases in the exit plane of the q rocket are variable since the geometry of the nozzle is still unsettled. However, the chamber properties have been given as:

1. Chamber Mach number = 0.10,
2. Chamber pressure = 172,800 lbs/sq ft,
3. Chamber temperature = 4500° Rankine,
4. Mass flow = 570 lbs/sec.

*These values were supplied by the Aerojet development group.

In order to compute the jet exit plane dynamic pressures it has been assumed that the exit plane Mach number will vary over the range $1.0 \leq M_e \leq 4.0$. The exit plane properties are calculated on the basis of an isentropic expansion between the stagnation values and the nozzle exit plane. The stagnation values are obtained by reducing the chamber values given at M = 0.10 to M = 0 by means of NACA Technical Note 1428.[2] The resulting stagnation values are listed as:

1. p_o = 174,100 lbs/sq ft,
2. T_o = 4520° Rankine,
3. ρ_o = 0.00625 slugs/ft^3.

The molecular weight of the exhaust gases has been assumed to be 8.5. Thus, the speed of sound corresponding to a molecular weight of 8.5 can be found from the speed of sound of air whose molecular weight is taken as 29 by the relation

$$\frac{c_\eta}{c} = \sqrt{\frac{29}{8.5}} = 1.846. \tag{4}$$

For a stagnation temperature of 4520°R the stagnation speed of sound for air would be

$$c_o = \sqrt{\gamma R T_o} = \sqrt{(1.4)(1715)(4520)} = 3293 \text{ ft/sec.} \tag{5}$$

The stagnation speed of sound in the η rocket case is then

$$c_{o_\eta} = c_o\,(1.846) = (3293)(1.846) = 6080 \text{ ft/sec.} \tag{6}$$

With the stagnation properties defined for the η rocket the static properties in the exit plane as a function of exit Mach number are computed with the aid of TN 1428.[2]

The calculations necessary to determine the exit properties for the η rocket are shown in Appendix B. The resulting values of $\left(V_e \sqrt{\rho_e/\rho_a}\right)_\eta$ and the scale factors corresponding to Equation 3 are given below.

(1)	(2)	(3)	(4)
M_e	$\left(V_e\sqrt{\frac{\rho_e}{\rho_a}}\right)_n$	$\left(V_e\sqrt{\frac{\rho_e}{\rho_a}}\right)_{Aerojet}$	Scale Factor
1.0	7710	2280	3.38
1.5	8310	2280	3.64
2.0	7580	2280	3.32
2.5	6420	2280	2.82
3.0	5240	2280	2.3
3.5	4235	2280	1.86
4.0	3450	2280	1.51

Column Explanation

(1) Assumed

(2) Appendix B, Table II

(3) From data given in text on Aerojet ambient air and exhaust properties

(4) Column (2)/Column (3) or Equation 3.

The above data indicate that the maximum exit dynamic pressure occurs at an exit Mach number of approximately 1.5 and yields a maximum scale factor of 3.64. Figure 10 represents a plot of the ratio of the maximum scale factor $\left(S_{M_e = 1.5} = 3.64\right)$ to the scale factor at any exit Mach number, $\left(S_{M_e}\right)$ as a function of exit Mach number.

THEORY

The flow external to the rocket exhaust boundaries must be one which can be satisfied by the existence of velocity potential since the physical processes involved in its formation are everywhere irrotational except in the region enclosed by the jet boundaries. These facts immediately suggest that the analytical treatment can be handled to a fair degree of approximation by perfect fluid theory. In addition, since the velocities are quite low (probably not exceeding 100 ft/sec in the region of interest) a further simplification can be made by assuming the induced flow to be incompressible. The assumption of an incompressible perfect fluid flow for the induced flow field implies the solution of Laplace's equation which is written as

$$\nabla^2 \varphi = \nabla^2 \psi = 0 \qquad (7)$$

where φ is the velocity potential, and ψ is the stream function.

Since the Laplace equation is linear, the principle of superposition can be employed and complex flow patterns can be built up by the linear addition of simple flows. A theorem,

[redacted]

[redacted]

concerned with incompressible perfect fluid flow, states that any complex flow which satisfies Laplace's equation can be built up with the proper combination of sources, sinks, and vortices. Thus, the problem of solving for the induced flow field about a rocket thrust chamber, external to the jet exhaust boundaries, resolves itself into finding the source, sink and vortex distributions which will satisfy a given set of boundary conditions. Before proceeding to the method of solution one further assumption was made. This involved the reduction of the problem from a three-dimensional flow to that of two dimensions. The reason for this added simplification is twofold. First, the use of two- instead of three-dimensional flow results in a stronger induced flow which is conservative for the present needs. It is felt that the uncertainty as to the correctness of the scale factor should be implemented in a conservative manner, thus the assumption of a two-dimensional flow. Further, the reduction from three- to two-dimensional flow has the added advantage of simplifying the mathematical model and the resulting equations which describe the flow.

A paper[3] by Squire investigates the case of a jet issuing into an airstream. In his work, Squire assumes the velocity profile at each jet cross section and shows that a sink distribution on the thrust axis that satisfies the inflow velocity across the jet boundary can be determined. Squire's assumed velocity profiles do not differ radically from limited experimental data, thus it is felt that a sink distribution on the thrust axis would prove to be satisfactory for qualitatively predicting the induced flow at large distances from the boundary of the jet. After studying the tuft results shown in Figs. 3 and 5 it appeared that the streamline directions indicated by the tufts might be fairly well described by a system of image sinks located on the thrust axis downstream of the nozzle exit plane. The necessity of image sink pairs is evident since a ground plane had to be simulated and this is conveniently accomplished by the use of an image system.

The equations[4] for an image sink pair are derived starting with the assumption that the origin of coordinates is defined by the intersection of the thrust axis and the ground plane. The positive X axis coincides with the thrust line and extends positively in the direction of the jet flow. The positive Y axis lies in the ground plane extending upward. To construct the image sink system, sinks are placed at $x = \pm a$ as shown below in Fig. 11.

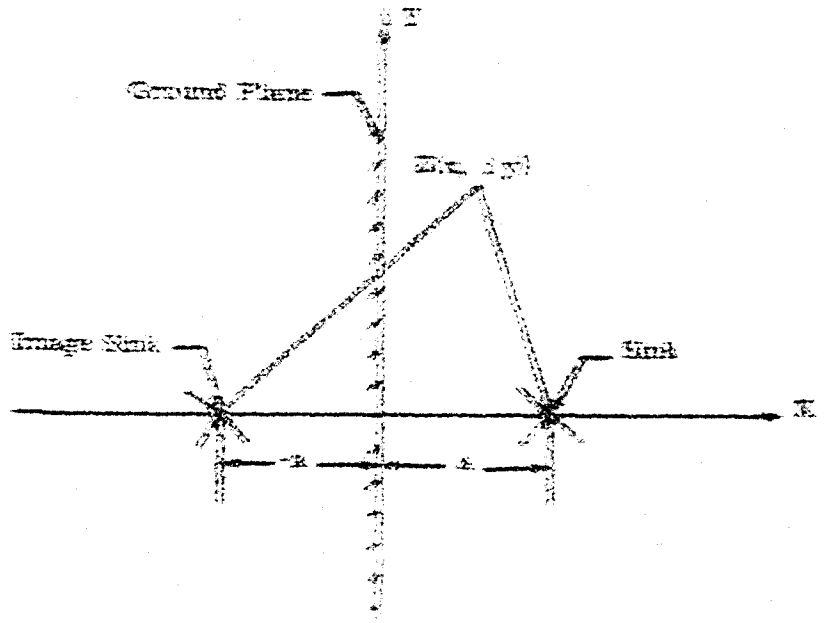

FIG. 11 IMAGE SINK SYSTEM

Let $Z = x + i\,y$ be any point in the complex plane. The complex potential, W, for an image sink pair is given[4] by

$$W = -\frac{m}{2\pi}\ln(z - a) - \frac{m}{2\pi}\ln(z + a) \tag{9}$$

where $W = \psi + i\,\phi$, m is the sink strength, and (a) is the distance from the origin to either sink. Simplifying Equation 9 we have

$$W = -\frac{m}{2\pi}\ln\left(z^2 - a^2\right). \tag{9}$$

The complex velocity, $u - i\,v$, is found by differentiation of the complex potential, W, with respect to z, that is

$$u - i\,v = \frac{dW}{dz} = -\frac{m}{2\pi}\frac{2z}{z^2 - a^2}. \tag{10}$$

By the use of partial fractions, Equation 10 is simplified to

$$u - i\,v = -\frac{m}{2\pi}\left\{\frac{1}{z - a} + \frac{1}{z + a}\right\}. \tag{11}$$

The denominators of the answer are made real by multiplying each by its conjugate.

$$u - iv = -\frac{m}{2\pi}\left(\frac{1}{z - z_1}\frac{\bar{z} - z}{\bar{z} - z} - \frac{1}{z - z_2}\frac{\bar{z} - z}{\bar{z} - z}\right) \tag{12}$$

where $\bar{z} = x - iy$.

Expanding z and $\bar{z}$ into their real and imaginary parts and grouping the real and imaginary parts of the right-hand side we get

$$u - iv = -\frac{m}{2\pi}\left[\left(\frac{x - z}{x^2 - 2xz + y^2 + z^2} - \frac{x - z}{x^2 + 2xz + y^2 + z^2}\right) - i\left(\frac{y}{x^2 - 2xz + y^2 + z^2} - \frac{y}{x^2 + 2xz + y^2 + z^2}\right)\right] \tag{13}$$

Let us now define

$$P = x^2 - 2xz + y^2 + z^2 \text{ and } Q = x^2 + 2xz + y^2 + z^2. \tag{14}$$

Substituting Equation 14 into Equation 13 and equating real and imaginary parts we have

$$u = -\frac{m}{2\pi}\left[P\left(\frac{1}{P} - \frac{1}{Q}\right) - z\left(\frac{1}{P} - \frac{1}{Q}\right)\right] \tag{15}$$

$$v = -\frac{m}{2\pi}y\left(\frac{1}{P} - \frac{1}{Q}\right). \tag{16}$$

In order to obtain an exact solution for the five experimental values of u and v determined in Appendix, Equations 15 and 16 are rewritten as

$$u_j = -\frac{1}{2\pi}\sum_{i=1}^{4} m_i\left[P_{ij}\left(\frac{1}{P_{ij}} - \frac{1}{Q_{ij}}\right) - z_i\left(\frac{1}{P_{ij}} - \frac{1}{Q_{ij}}\right)\right] \tag{17}$$

$$v_j = \frac{1}{2\pi}\sum_{i=1}^{4} m_i y_j\left(\frac{1}{P_{ij}} - \frac{1}{Q_{ij}}\right) \tag{18}$$

where the subscript "i" represents summation over the five sinks and their images and the subscript "j" represents the magnitudes of the measured velocities and their field locations. The solution of Equations 17 and 18 requires the solution of an simultaneous equations which are linear in the m_i but nonlinear in the z_i. Programs for the CRAY DMA and Remington Rand 1107A were set up and run but the processes tried in these programs failed to converge. Subsequent analytical juggling of the equations resolved themselves into the solution of a quintic

whose five roots had to be real for an exact solution. It was shown that three of the roots were real but a complex pair also existed. Thus, the search for an exact solution was abandoned. An approximate solution[5] was then undertaken. This solution[5] involved a program on the CRC 102A wherein a single sink and its image were placed on the thrust axis so as to yield a minimum velocity $\left(\sqrt{u^2 + v^2}\right)$ difference between the five experimental and corresponding theoretical values when this error was summed over the five points. After finding the optimum position and strength for the first image sink pair, a second image sink pair was added and its position and strength were varied (holding the strength and position of the first pair constant) until the error was again minimized. The strength and position of the first pair (holding the second pair constant) were then altered until the velocity error was again minimized. This iterative procedure was continued until a minimum error resulted. The difference flow between the two sink pairs and the experimental values indicated that a third sink pair would add little or nothing to the velocity error since the difference flow could not be simulated by additional sink or source pairs.

RESULTS

The computations on the CRC 102A computer indicate that the best fit to the experimental data using image sources and sinks located on the thrust axis are as follows:

1. Sink of strength, $m = -400\ ft^2/sec$ located at $x = \pm 2.78$ feet,
2. Source of strength, $m = 308\ ft^2/sec$ located at $x = \pm 2.88$ feet.

A comparison of the measured velocities and those calculated by the image sources and sinks listed above is summarized below.

Probe No.	Probe Locations x (ft)	Probe Locations y (ft)	Measured Velocities u (ft/sec)	Measured Velocities v (ft/sec)	Calculated Velocities u (ft/sec)	Calculated Velocities v (ft/sec)
1	1.98	0.52	20.4	-24.4	20.3	-20.4
2	1.98	0.792	8.0	-17.8	11.7	-21.5
3	1.98	1.052	6.1	-11.5	6.3	- 2.0
4	0.99	0.625	12.5	-12.5	7.8	- 6.6
5	0.99	0.875	7.8	-12.0	5.1	- 6.7

Examination of the data tabulated above indicates that the agreement is quite reasonable at probe positions 1 and 2. At positions 3, 4, and 5 the measured velocities are above and below the calculated values so that an averaging process indicates that the errors are not too large. On the basis of this data, although qualitative in agreement, it was decided that

velocities at other field points, including the ground plane, could be predicted to the correct order of magnitude using the source and sink locations derived from the CRC 102A computer. Since the source and sink locations on either side of the ground plane differ by only 0.1 feet and the field points in the vicinity of the ground plane are at least 2.78 feet from the sink, a further simplification for ease in computational procedure was incorporated. It was assumed that the source and sink on either side of the ground plane could be lumped together thus giving a single image sink pair whose strength is $m = -172\ ft^2/sec$ and located at $x = \pm 2.78$ feet. In order to further check the assumption of a single image sink pair the streamline directions were computed for an image sink pair located at $x = \pm 2.86$ $\left(\frac{x}{d_e} = \pm 5.5\right)$. The discrepancy between the predicted value of $x = \pm 2.78$ and $x = \pm 2.86$ resulted from the fact that streamline patterns had been computed at values of $\frac{x}{d_e} = \pm 1$, 1.5, and 2.0 prior to the program on the CRC 102A. However, the discrepancy between the $x = \pm 2.86$ feet and $x = \pm 2.78$ feet locations would produce negligible changes in velocity at distant field points. The streamline patterns predicted by the single image sink system and the tuft data shown in Fig. 5 are plotted in Fig. 12. The agreement is fairly good and qualitatively substantiates the assumption that a single image sink pair can be used to predict velocities at various field points as well as on the ground plane. Thus, with the image sink strength and location given by the CRC 102A computer, various field and ground plane velocities (including velocity direction) were computed. The results of these computations are plotted in Figs. 13 and 14. The data in Fig. 13 are shown for values of $4 \le \frac{x}{d_e} \le 0$ and $0 \le \frac{y}{d_e} \le 10$, while the data in Fig. 14 represent the data for $0 \le \frac{x}{d_e} \le 4$ and $0 \le \frac{y}{d_e} \le 100$. The velocity magnitudes in Figs. 13 and 14 were computed using the maximum scale factor of 3.64 which occurs at a nozzle exit plane Mach number of 1.5. The data can be applied to any exit plane Mach number between unity and four by multiplying the length of each velocity vector by the appropriate value of the scale factor found in Fig. 11. The flow directions are assumed to be invariant with variations in nozzle exit plane Mach number. Speculation might arise as to the effect of the nozzle exit plane flow if it be under- or over-expanded. This effect has not been considered because of a lack of data and a lack of time. However, it is felt that the combination of conservative scale factors and the assumption of two-dimensional flow will probably offset the effects of under- or over-expansion of the nozzle flow.

CONCLUSIONS

The data derived in Figs. 13 and 14 will indicate the size of concrete pad required once the allowable ground velocity magnitude is ascertained. The data will also predict, in the vicinity of the test stand, the local velocities to which instrumentation will be subjected. It is felt that the velocity predictions shown in Figs. 13 and 14 are correct in order of magnitude and should not exceed the values shown if the chamber conditions are maintained at the

[redacted]

[redacted]

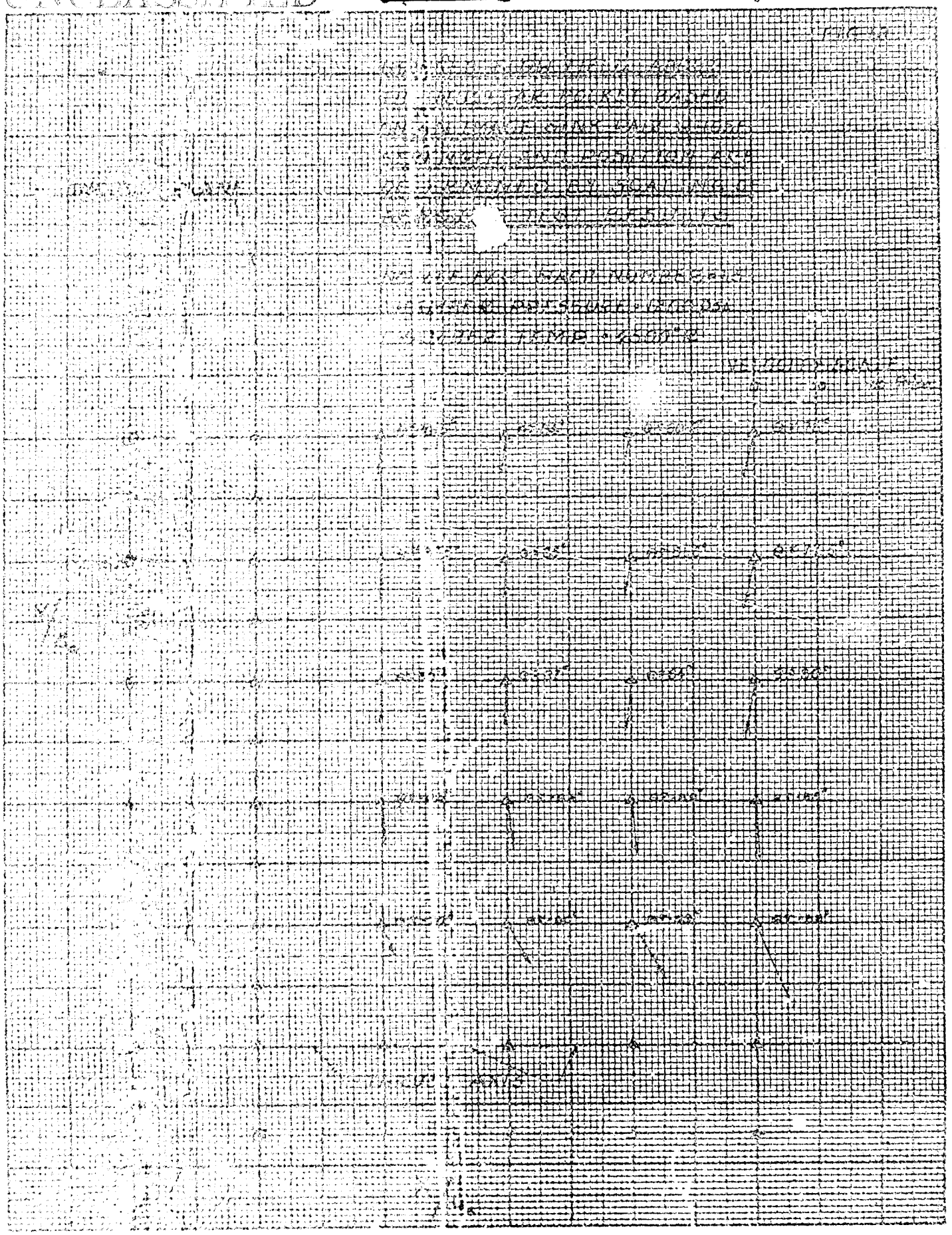

[redacted]

[redacted]

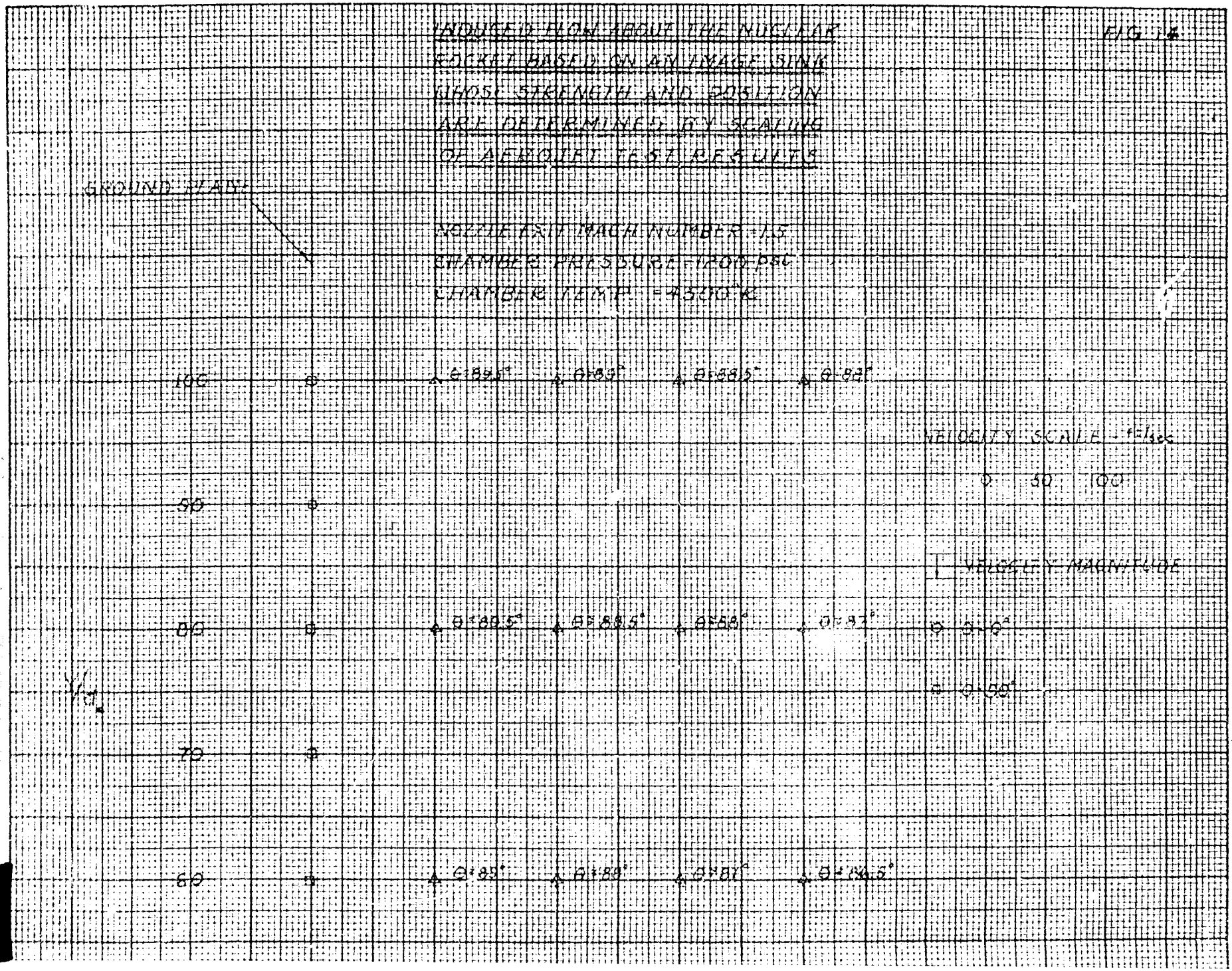

[redacted]

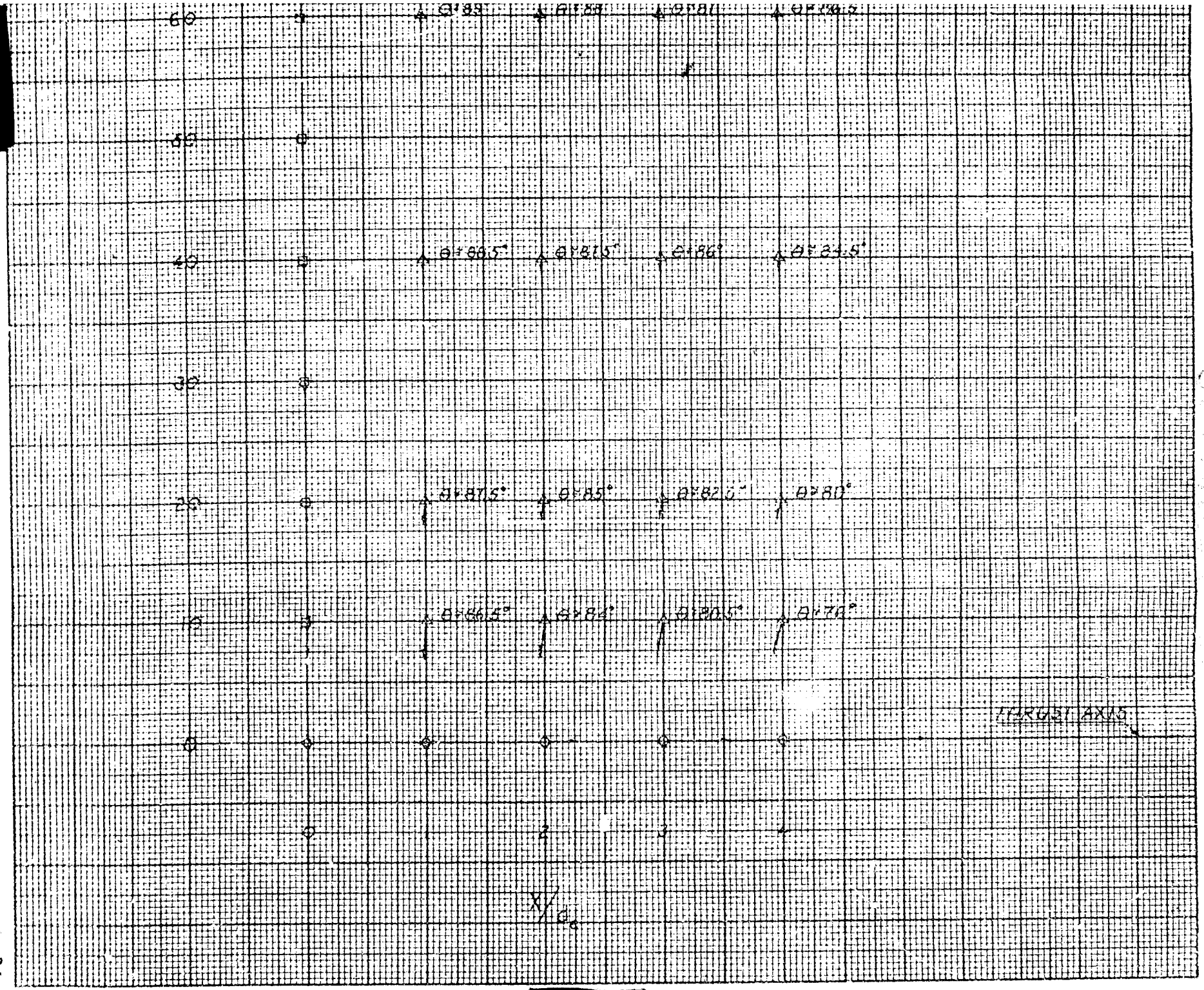

Ref. Sym: 5141 (607)

values reported herein. For higher values of stagnation pressure and stagnation temperature the magnitude of the induced flow will increase and vice versa.

It should be realized that the data presented herein represent a "best guess" based on limited experimental evidence and on an approximate analytical extropolation of the experimental data.

ARNOLD L. DUCOFFE

FRED G. BLOTTNER - 5141

V. T. STRASCINA - 5142

W. E. WALKER - 5143

Case No. 409.10
January 2, 1957

APPENDIX A

TABLE I

Run Program at Aerojet Using a 2600-Pound Nike Thrust Chamber

Run No.	Comments
1	Tuft study with ground plane 54 inches forward of the nozzle exit plane (see Figs. 2 and 3).
2	Flow study using titanium tetrachloride vapors to give flow directions above the thrust chamber (see Fig. 8). A fairing covering the top of the thrust chamber was added.
3	Pressure measurements using 5 pitot-static tubes located above the thrust chamber and one flush static orifice located in the ground plane 54 inches above the thrust axis in the vertical plane containing the thrust axis (see Fig. 6). Pressure data was not obtained because camera photographing the manometer board (inclined at 15°) failed.
4	Rerun of Run 3. Data good.
5	Ground plane moved to a position 24 inches forward of nozzle exit plane. Flush static orifices 18 inches and 36 inches above thrust axis in the vertical plane containing the thrust axis were installed. Pitot tubes in same location as Run 3.
6	Tuft studies with ground plane in 24-inch position (see Figs. 4 and 5).

APPENDIX B

TABLE II

Scale Factors for the Induced Flow Field Created by the Nuclear Rocket Exhaust

(1) M_e	(2) $\frac{p_e}{p_o}$	(3) $p_e \times 10^{-3}$	(4) $\frac{\rho_e}{\rho_o}$	(5) $\rho_e \times 10^{3}$	(6) $\frac{T_e}{T_o}$	(7) $T_e \times 10^{-3}$	(8) $\frac{c_e}{c_o}$	(9) $c_e \times 10^{-3}$	(10) $\frac{A^*}{A_e}$
1.0	.528	91.9	.634	3.96	.833	3.77	.913	5.56	1.000
1.5	.272	47.3	.395	2.47	.690	3.12	.831	5.06	.850
2.0	.128	22.3	.230	1.44	.556	2.51	.745	4.53	.593
2.5	.0585	10.18	.132	.825	.444	2.01	.667	4.06	.380
3.0	.0272	4.73	.0762	.476	.357	1.62	.598	3.64	.234
3.5	.0131	2.28	.0460	.282	.290	1.31	.538	3.27	.142
4.0	.00659	1.147	.0277	.173	.238	1.08	.485	2.97	.0933
(12)	(13)	(13)	(14)	(15)	(16)	(17)	(18)	(19)	(20)
M_e	A_e	A_o	d_o (ft)	$V_e \times 10^{-3}$	$\frac{\rho_e}{\rho_a}$	$\frac{\rho_e}{\rho_a}$	$\left(V_e\sqrt{\frac{\rho_e}{\rho_a}}\right)_o$	$\left(c_o\sqrt{\frac{\rho_e}{\rho_a}}\right)_o$ Aerojet	Scale Factor
1.0	.546	.730	.884	5.56	1.023	1.387	7710	2280	3.38
1.5	.642	.800	.906	7.59	1.20	1.095	8310	2280	3.64
2.0	.921	.960	1.063	9.08	.699	.818	7680	2280	3.32
2.5	1.440	1.200	1.350	10.15	.40	.643	6430	2280	2.82
3.0	2.310	1.520	1.720	10.92	.231	.480	5240	2280	2.30
3.5	3.710	1.930	2.170	11.45	.137	.576	4235	2280	1.86
4.0	5.85	2.420	2.730	11.09	.084	.390	3450	2280	1.51

APPENDIX C

CALIBRATION OF A STATIC PROBE AS A FUNCTION C[illegible]NGLE OF ATTACK

The tuft data in Figs. 3 and 5 indicate that the flow angles [illegible] vicinity of the static ports varied from approximately 45 to 60 degrees. Published [illegible] on static errors as a function of angle of attack are limited to angles of attack betw[illegible] and 30 degrees at speeds above 50 feet/second. In order to interpret the static pressure[illegible] measured at Aerojet it became necessary to calibrate a static probe at angles of attack [illegible]ess of 30 degrees. A static probe calibration program was conducted in the Sandia [illegible] free jet wind tunnel. The probe was constructed from steel t[illegible] on 8-inch diameter in diameter. A hemispherical nose was welded on the front e[illegible] measured 1/4-inch holes placed 2 inches (or 8 diameters) behind the shoulder fo[illegible] be and the static hemispherical nose and the cylindrical afterbody. The [illegible] by the function of the angle-of-attack range between 0 and 65 degrees at speeds varying b[illegible] induced over an angle- [illegible] 5 and 50 feet/second. The procedure consisted of setting the probe in the free jet [illegible] the tunnel horizontal axis and then rotating the probe about the static hole [illegible] 65 degrees. A constant tunnel speed was maintained for each set of [illegible] Static pressures were measured by means of an alcohol U-tube which [illegible] atmosphere. For added sensitivity the U-tube was tilted at an angle [illegible] degrees [illegible] the horizontal. Since the free jet is at atmospheric pressure (for [illegible] the U-tube gave a zero reading when the probe was aligned with the [illegible] axis. As [illegible] probe was rotated through the angle-of-attack range static pressures corresponding to [illegible] probe angle were read and recorded.

The results of these tests are presented in Fig. 15 wher[illegible] plot of static pressure error (Δp in lbs/sq ft) versus probe angle with [illegible] speed as a [illegible]meter is shown. The data indicate that the measured pressure is lower than the [illegible] pressure. Also it is noted that the error for a given velocity reaches a maximum [illegible] roximately 60 degrees angle of attack, then starts to decrease. In order to apply this [illegible] to the measured static pressures at Aerojet requires an iterative procedure. Given a [illegible] asured pressure and a total head pressure a velocity is computed from the Bernoulli e[illegible]ation,

$$p + 1/2\ \rho V^2 = H$$

where H is the total head pressure. With the calculated velocity [illegible] the flow inclination a static pressure error is found from Fig. 15. A corrected static [illegible] ssure is computed from the measured static pressure and the static pressure error and [illegible] w velocity computed. A

[redacted]

FIG 18

STATIC PRESSURE ERROR
AS A FUNCTION OF FLOW
INCLINATION AND VELOCITY
ON A 1/4" STATIC PROBE

ΔP = MEASURED - ACTUAL STATIC PRESSURE

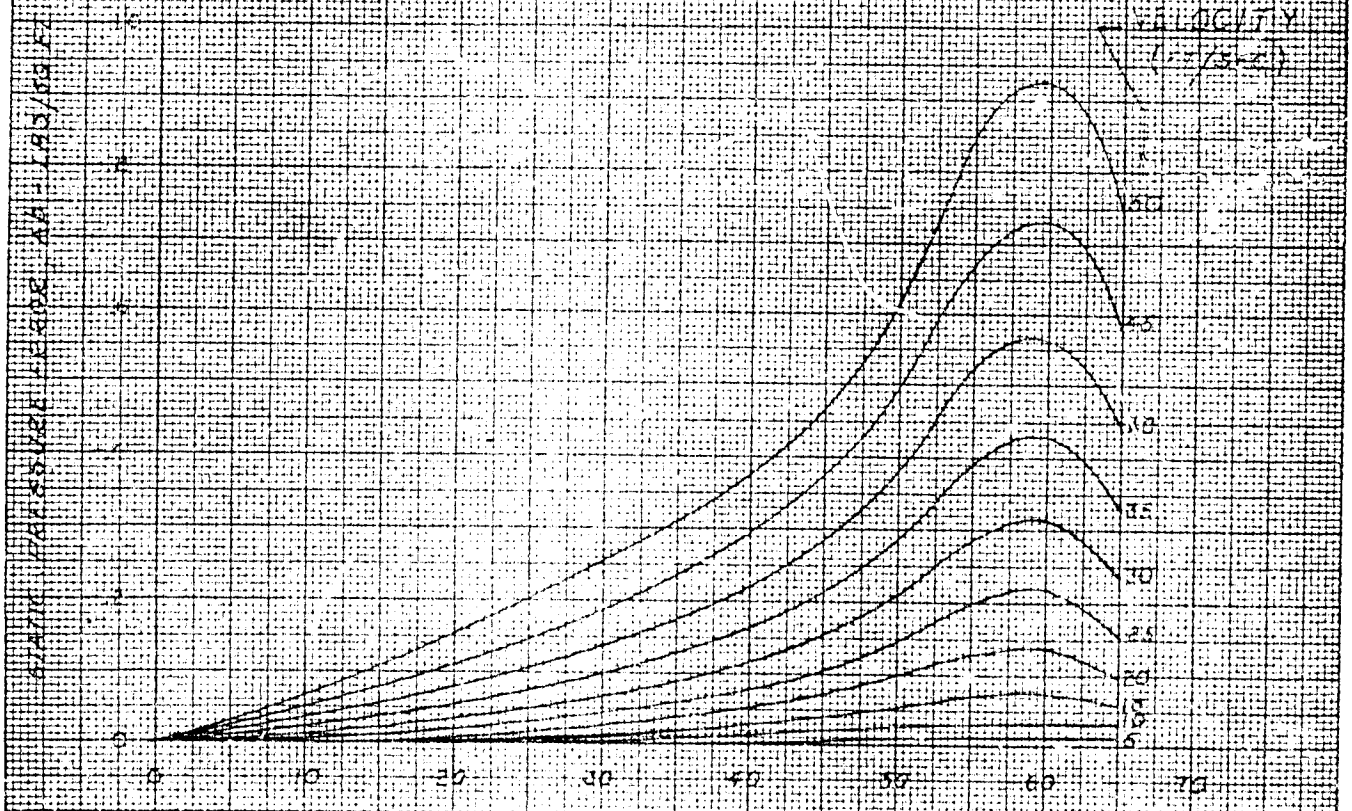

[redacted]

new static pressure error is found from Fig. 15. The process is repeated until the difference between the nth and $n + 1^{th}$ computed velocities is essentially zero or to any order of accuracy desired. The process converges quite rapidly and requires only two or three iterations.

UNCLASSIFIED

BIBLIOGRAPHY

1. Stratford, B. S., "Mixing and the Jet Flap", The Aeronautical Quarterly, Volume VII, pp. 92-95, May 1956.

2. Staff of the Ames 1- by 3-Foot Supersonic Wind Tunnel Section, Notes and Tables for Use in the Analysis of Supersonic Flow, NACA TN 1428, December 1947.

3. Squire, H. B. and Trouncer, J., Round Jets in a General Stream, Aeronautical Research Council Reports and Memoranda 1974, January 1944.

4. Milne-Thomson, L. M., Theoretical Hydrodynamics, The MacMillan Co., Chapter VIII, 1950.

5. Morrison, D. R. and Kleinecke, D. C., Fitting Flow Data with a Radial Flow, Sandia Corporation TM 182-56-51, to be published.

6. Pankhurst, R. C. and Holder, D. W., Wind Tunnel Technique, Sir Isaac Pitman and Sons, Ltd., pp. 184-190, 1952.